A Final Report to NASA for the SUNLITE Program

Sub-Hertz relative frequency stabilization of two diode laser pumped Nd:YAG lasers locked to a Fabry-Perot interferometer

Professor R. L. Byer

Edward L. Ginzton Laboratory

Stanford University

Stanford, California 94305

(415) 723-0226

Abstract

Two diode laser pumped Nd:YAG lasers have been frequency stabilized to a commercial 6.327 GHz free spectral range Fabry-Perot interferometer yielding a best case beatnote linewidth of 330 mHz. In addition, a Fabry-Perot interferometer with a free spectral range of 680 MHz, a linewidth of 25 kHz and a finesse of 27,500 has been built and when it was substituted in place of the commercial interferometer produced a robust and easily repeatable beatnote linewidth of 700 mHz.

Sub-Hertz relative frequency stabilization of two diode laser pumped Nd:YAG lasers locked to a Fabry-Perot interferometer

I. Introduction

Diode laser pumped solid state lasers are efficient all solid state sources of coherent radiation[1,2] that have applications in spectroscopy,[3] coherent communication,[4,5] laser radar[6] metrology,[7] clocks,[7] gravity wave astronomy,[8,9] harmonic generation,[10] parametric oscillation[11] and squeezed state generation.[12] Several of the more interesting applications for frequency stabilized lasers, including low frequency gravity wave detection[13] and microarcsecond astrometry[14] will require highly coherent lasers frequency stabilized to interferometers in space. As preparation for these and other space-based optical experiments,[15] a space qualified version of the experiment discussed in this paper is currently being developed by NASA Langley for a space shuttle flight in 1994 under the SUNLITE program.[16] This paper describes work leading to the 330 mHz relative frequency stabilization of two diode laser pumped Nd:YAG laser achieved by actively locking to an external Fabry-Perot reference interferometer.

Active frequency stabilization of a diode laser pumped Nd:YAG laser to a high finesse Fabry-Perot interferometer using feedback was initiated at Stanford in 1988.[7] Because of the engineering difficulty and cost associated with the seismic and acoustic isolation of separate reference interferometers for locking independent laser oscillators,[17] advantage was taken of the common mode rejection available by independently locking two diode laser pumped Nd:YAG lasers to adjacent axial modes of the same Fabry-Perot interferometer. The two lasers, independently stabilized with their own servos to adjacent axial modes of the same interferometer, are well outside of their mutual injection locking range and thus the beatnote linewidth between the two lasers is a measure of how well each laser remains locked to its respective Fabry-Perot axial mode.

The diode laser pumped nonplanar ring oscillator (NPRO) was invented in 1985 by Kane and Byer.[18] The inherent short term frequency stability of the NPRO was demonstrated in 1987 when

Kane measured a beatnote linewidth of 10 kHz between one NPRO and a monolithic standing wave laser.[19] The measurement was made by spectral analysis of the 17 MHz beatnote between the two lasers whose difference frequency was controlled with a low bandwidth servo to remove slow frequency drifts. In 1987 Nilsson began active wide band stabilization of these lasers by fringe side locking two low power (2 mW) Nd:GGG NPROs to a Coherent Radiation Inc. Model 216-G confocal interferometer with a finesse of 300, a free spectral range of 300 MHz and an optical bandpass of 1 MHz.[20] The heterodyne beatnote of these two lasers was measured to have a linewidth less than the spectrum analyzer resolution of 511 Hz.[7] In 1988 Day improved the experiment using Pound-Drever locking and a commercial (Newport SuperCavity Model SR-150-C) high finesse reference cavity with a finesse of 22,000, a free spectral range of 6.327 GHz and an optical bandpass of 288 kHz. A beatnote linewidth of 30 Hz resulted.[21] This was followed in 1989 by improvements to the servo and the optomechanical mounts that produced a 3 Hz heterodyne beatnote linewidth.[22] In 1990 the 2 mW Nd:GGG NPROs were replaced with 40 mW Nd:YAG NPROs and an acoustooptic modulator was added to provided additional optical isolation. These modifications reduced the beatnote linewidth further to the 330 mHz result reported here.

II. Theory of laser frequency stabilization to an interferometer

Laser frequency stabilization can be treated as a problem in control theory.[23] Figure 1 is a schematic of a laser frequency stabilization control problem. The laser is modeled as the plant with an output frequency, ν, which is perturbed by some noise process $S_{f,laser}$ where $S_{f,laser}$ is the linear spectral density of frequency noise associated with the laser and is a measure of the rms laser frequency fluctuation in a 1 Hz bandwidth. It therefore has units of $Hz/\sqrt{Hz}$ and is frequency dependent in a diode laser pumped solid state laser with most of the frequency noise below 1 kHz.[24]

The instantaneous frequency of the laser is monitored with a discriminator which converts the optical frequency fluctuations into voltage fluctuations with a conversion gain or slope of

D_v(V/Hz), thus producing an error signal. This error signal is amplified and compensated in the servo which has a frequency dependent gain coefficient G(V/V). The amplified voltage fluctuations are then fed back negatively to the actuator which converts them into frequency fluctuations with a conversion gain K(Hz/V). In this way the control loop monitors and actively suppresses the frequency noise of the laser. Sources of frequency noise in diode laser pumped solid state lasers the implementation of the control loop (frequency discriminator, servo and frequency actuator), and the frequency noise suppression that can be achieved with the control loop are discussed in the next three sections.

A. Control Theory

There are several noise processes which perturb the frequency of the laser and lead to a laser output that is not a single perfect sinusoid. The most fundamental of these noise processes is the Schawlow-Townes or quantum noise limit which results from spontaneous emission perturbing the phase of the carrier field in a random fashion. The spectral density of frequency noise, $S_{f,ST}$(Hz/$\sqrt{\text{Hz}}$), associated with this quantum noise process is white with a magnitude given by[25]

$$S_{f,ST} = \delta\nu_L\sqrt{\frac{2h\nu}{P}} \qquad (1)$$

where $\delta\nu_L$ is the laser cold cavity linewidth and P is the laser output power. An oscillator with a white spectral density of frequency noise, S_f, has a 3 dB linewidth, $\Delta\nu$, given by (Elliot 1982)

$$\Delta\nu = \pi S_f^2 \quad . \qquad (2)$$

The Schawlow-Townes limited laser linewidth, $\Delta\nu_{L,ST}$, is therefore

$$\Delta\nu_{L,ST} = \pi S_{f,ST}^2 = \frac{2\pi h\nu\delta\nu_L^2}{P} \quad . \qquad (3)$$

This quantum limited linewidth can be as low as 1 Hz for output powers of 1 mW in a diode laser pumped Nd:YAG laser because of the low crystal loss and resultant very narrow laser cavity linewidth.[27]

Diode laser pumped solid state lasers achieve this level of performance only at frequencies above 100 kHz. Below 100 kHz pump laser amplitude fluctuations, which disturb the optical path length of the solid state laser, produce excess frequency noise.[24] This noise source typically has a spectral density of frequency noise which varies as $(1/f)^a$ and is much greater than the quantum limit at low frequencies. However, this frequency noise is detected by the frequency discriminator and may be suppressed by a feedback control system.

The frequency discriminator must provide an output voltage linearly proportional to the optical frequency fluctuations of the laser. There are several techniques for accomplishing this task. The most common is to compare the frequency of the laser to a standard and use the difference frequency between the two as the error signal. The standard can be another laser or an optical resonance which, if it is not itself a standard, can be locked to one. In coherent communications experiments the difference frequency (heterodyne) or the difference phase (homodyne) between two or more sources is held constant leading to similar control requirements.[5,28] Since it is the difference frequency or phase which is controlled in each of these techniques, relative stabilization is the end result. However, if it is necessary, the stability of the standard, the resonance, or the additional source can also be controlled, leading to the absolute stability of the plant. In practice this is difficult for many reasons including the ambient environmental noise. The properties of the frequency discriminant usually determine the overall performance of the control loop.[29]

An optical interferometer provides an effective technique to obtain fast frequency discrimination.[30,31] In this technique the instantaneous frequency of the laser is compared to the resonance frequency of the interferometer and an error signal proportional to the difference is generated. The two most common methods by which the error signal is generated are the fringe side locking [30,32-34] and the Pound-Drever locking techniques.[31]

In fringe side locking the frequency of the laser is locked in transmission to the half power point of a high finesse interferometer. At the half power point the interferometer output power is linear in laser frequency deviation for small fluctuations and the slope is a maximum. To increase the discriminator slope, D_V(V/MHz), it is necessary to decrease the interferometer optical linewidth. There is an increased time delay associated with transmission through the higher resolution cavity, however, and frequency fluctuations occuring at rates fast compared to the inverse of the cavity linewidth produce a greatly reduced error signal together with a time delay in the control loop.[33] Furthermore, locking on the side of the cavity transmission fringe requires amplitude noise suppression because low frequency fluctuations in the amplitude of the laser are interpreted by the servo as frequency fluctuations and hence are fed back to the actuator producing frequency noise. A technique that overcomes both of these difficulties is known as Pound-Drever locking.[31]

A schematic diagram for the Pound-Drever type of frequency discriminator is illustrated in Figure 2. The laser is mode matched to the high finesse interferometer and phase modulated at an RF frequency, ω_m, which is large compared to the interferometer optical bandwidth. The phase sidebands of the laser are therefore reflected from the interferometer with no relative phase shift and are focused onto a high speed photo-diode. Near resonance the reflected carrier experiences a strongly dispersive phase shift.[35] When the phase shifted carrier is mixed with its sidebands on the photo-diode an amplitude modulated term at the modulation frequency is created with an amplitude proportional to the sine of the round trip phase shift (θ). Near resonance this term is linearly proportional to the frequency offset; $\sin\theta \sim \theta = 2\pi\delta\nu_{l\text{-}c}/\mathrm{FSR}$ where FSR is the cavity free spectral range and $\delta\nu_{l\text{-}c}$ is the difference between the laser frequency and the cavity resonance frequency.[25] The discriminant arises because a nonzero phase shift on the carrier no longer allows the mixing products (ω_o, $\omega_o + \omega_m$) and (ω_o, $\omega_o - \omega_m$) to perfectly cancel, as is the case for purely phase modulated light, thus producing an amplitude modulation.

The error signal is obtained by mixing a portion of the RF drive used to phase modulate the laser with the output of the photo-diode. A low pass filter is then used to detect only the envelope

of the AM term which carries the frequency noise information of the laser. An additional benefit of this phase sensitive detection at the RF modulation frequency is that the system is immune to low frequency amplitude noise on the laser output. The system is, however, limited by amplitude noise on the laser beam at the modulation frequency. For this reason the phase modulation of the laser field is at a frequency that is shot noise limited in amplitude. In addition, the frequency response and electronic bandwidth of the Pound-Drever error signal are greater than those of fringe side locking. (A derivation of the slope of the Pound-Drever error signal together with its frequency dependence are calculated in appendix A.) This increased response results because the reflected field carries information on the instantaneous frequency of the laser, as well as the phase history of the laser, and therefore delays associated with the interferometer buildup time are eliminated. Although Pound-Drever locking is more difficult to implement than fringe side locking, the advantages of wide bandwidth frequency control and improved low frequency amplitude noise rejection make it an increasingly popular frequency discriminator.

The output of the frequency discriminator is amplified and shaped by the servo whose output subsequently drives the frequency actuator. In low bandwidth control systems the discriminator and actuator typically have flat frequency responses across the loop bandwidth and therefore, the response of the servo determines the overall frequency response of the controller.

In our experiment the servo gains, G, approached 120 dB at low frequencies. This was necessary to suppress the large 1/f component in the spectral density of laser frequency noise to a level below the Schawlow-Townes quantum limit. Diode laser pumped solid state lasers typically become quantum limited in frequency noise at 100 kHz and therefore unity gain frequencies of 100 kHz are adequate. The low bandwidth dramatically simplifies loop construction and is a direct result of the passive frequency stability of diode laser pumped solid state lasers. The loop bandwidth is more than an order of magnitude smaller than that required in servos meant to control dye lasers or diode lasers.[29,36] The gain rolls off with a slope of 12 dB/octave in order to maintain this low loop bandwidth and a lead stage is used in the servo to maintain the proper slope of 6 dB/octave at the unity gain point. The output of the servo drives the frequency actuator.

The frequency actuating element in the control loop converts the voltage fluctuations from the servo into frequency fluctuations of the laser. There are several ways this can be accomplished in nonplanar ring oscillators. Temperature control of the laser gain medium controls the optical path length of the laser and therefore its frequency. However, temperature control is slow (~1 Hz) and cannot respond to the fast frequency fluctuations observed in the output of diode laser pumped solid state lasers. Control of the current supplied to the diode laser pump also allows frequency control of the laser. Modulation of the pump laser current modulates the pump power and therefore the temperature of the NPRO mode volume. This is, therefore, the same as temperature control of the laser frequency. However, because the volume being controlled in this manner is small, the response can be fast (~1 kHz). The response of this technique however, is still not fast enough to suppress the frequency noise over a wide band. Furthermore, modulating the current has the undesirable effect of modulating the amplitude of the laser.

The most attractive alternative to these techniques, and the technique used in this work, is to control the optical path length of the Nd:YAG laser resonator using piezo-electric transducers (PZTs). A PZT is bonded to the top, non-optical face of the nonplanar ring oscillator and an applied voltage modulates the optical path length and therefore the frequency of the laser. The laser gain medium is no more than 3 mm thick and the frequency response is typically flat to 200 kHz with an actuating coefficient, K(MHz/V), of between 0.5 and 5.0 MHz/V. The frequency discriminator, servo and frequency actuator constitute the control loop which is used to actively suppress the free running frequency noise of the laser.

B. Frequency noise reduction by active control

Using active frequency control the spectral density of laser frequency noise, $S_{f,\,laser}$, can be suppressed over the bandwidth of the control loop. The closed loop spectral density of frequency noise, $S_{f,cl}(Hz/\sqrt{Hz})$, for the control problem shown in Figure 1, where the discriminator noise and servo noise, are ignored is given by

$$S_{f,cl} = \frac{S_{f,laser}}{|1 + KGD_v|} \quad . \tag{4}$$

where K is the actuator coefficient, G is the servo gain, and D_v is the discriminator slope as defined earlier. This equation is crucial to the understanding of the frequency noise reduction that can be achieved when using active frequency control. However, it represents a somewhat simplified view of active frequency control because it assumes that the closed loop performance is affected only by the frequency noise of the laser. This is difficult to realize in practice. A more realistic situation is one where each element in the controller is modeled to have a noise contribution which adds to its output.

The laser and actuator noise contributions are combined in Figure 1 into one term, $S_{f,laser}$, because the noise contribution at the output of the actuator is indistinguishable from the laser noise. $S_{v,disc.}$ and $S_{v,servo}$ are the spectral densities of voltage noise associated with the frequency discriminator and servo. These spectral densities have units of $V/\sqrt{Hz}$ and represent the rms voltage fluctuation in a 1 Hz bandwidth at the corresponding control element output . The closed loop spectral density of frequency noise in the presence of these excess noise terms can be derived by analyzing the contribution from each term separately. The linear spectral density is the square root of the power spectral density and the total noise power is the sum of the individual contributions. Therefore, the total closed loop linear spectral density of frequency noise is given by

$$S_{f,cl} = \frac{\sqrt{S_{f,laser}^2 + |KS_{v,servo}|^2 + |KGS_{v,disc}|^2}}{|1 + KGD_v|} \quad . \tag{5}$$

In the limit of very large servo gain, G, the discriminator noise contribution dominates all other terms and the minimum closed loop spectral density of frequency noise is

$$S_{f,cl\ min} = \frac{S_{v,disc.}}{D_v} \quad . \tag{6}$$

This minimum spectral density of frequency noise depends only on the properties of the discriminator, D_v, and its noise contribution, $S_{v,disc.}$. The discriminant noise, however, includes contributions from technical noise associated with the discrimination technique such as fluctuations in the resonant frequency of the Fabry-Perot, 1/f noise in the discriminant amplifiers and quantum noise associated with measurement of the laser frequency. For a properly designed frequency controller the fundamental limit on frequency noise is set by the quantum fluctuations at the discriminant detector. The slope of the frequency discriminator (derived in the appendix A) together with the quantum fluctuations at the discriminant detector therefore determine the overall performance limit. It is for this reason that the discriminator is such a critical element in the control loop. The quantum limit on frequency noise reduction is derived in the next section.

C. Quantum limited frequency noise reduction

With sufficient servo gain the minimum closed loop spectral density of laser frequency noise is determined by the discriminator slope and noise spectral density. The slope of the discriminator is given in the appendix in equation A.14. In an optimally designed controller the discriminator spectral density is determined by the quantum limited shot noise on the photo-detector output. Equations A.4 and A.5, however, demonstrate that on resonance in an impedance matched cavity ($R_1 = R$; $F(0) = 0$), only the DC contribution from the sideband power, $2J_1^2(\beta)P_i$, contributes to the shot noise at the photo-detector. Therefore, the discriminator shot noise spectral density of current, $S_{A,disc}(A/\sqrt{Hz})$, associated with this power level is given by [25]

$$S_{A,disc}(A/\sqrt{Hz}) = \sqrt{2}\,\sqrt{2eI} = \sqrt{2}\,\sqrt{2e\left(2J_1^2(\beta)\frac{e\eta P_i}{h\nu}\right)}\,, \qquad (7)$$

where I is the detector photo-current induced by the DC power level, $2J_1^2(\beta)P_i$, η is the quantum efficiency, and hv is the energy of the detected photons. The additional factor of $\sqrt{2}$ comes from noise in the upper and lower sidebands which are mixed down to the same positive frequency and add incoherently. Equations (A.14) and (7) can be substituted into equation (6) to obtain the

minimum closed loop spectral density of frequency noise due to these frequency discriminator quantum limited amplitude fluctuations:

$$S_{f,cl\ min}(Hz\sqrt{Hz}) = \frac{\delta\nu_c}{J_0(\beta)}\sqrt{\frac{h\nu}{8\eta P_i}} \quad . \tag{8}$$

Equation 8 can now be combined with equation 2 to obtain the minimum laser linewidth

$$\Delta\nu_{L\ min} = \frac{2\pi\, h\nu\, \delta\nu_c^2}{16\,\eta P_i\, J_0^2(\beta)} \quad . \tag{9}$$

A comparison of equation 9 with equation 3 demonstrates that the closed loop, shot noise limited laser linewidth is equal to the Schawlow-Townes limited linewidth with $\delta\nu_L$ and P replaced by $\delta\nu_c$ and $16J_0^2(\beta)\eta P_i$ respectively. As a result, with very narrow discriminator linewidths (large D_ν, $D_{A,}$) the closed loop spectral density of frequency noise can be suppressed to a level below the Schawlow-Townes limit within the bandwidth of the loop.

The term $16J_0^2(\beta)$ is an efficiency factor resulting from the Pound-Drever frequency discriminator and does not appear in the analysis of Salomon et al.[29] For $\beta = 1.08$ (the optimum value for the discriminator slope is discussed in appendix A.) this term leads to a linewidth reduction of ~8.5 as compared to frequency stabilization techniques based on transmission locking.[29] Stabilization experiments using transmission locking therefore require greater than eight times the optical power to achieve the same level of shot noise limited frequency stability as in the impedance matched reflection locking technique. This enhancement in performance is due to the increased slope associated with the Pound-Drever technique, as shown in equation A.13, as well as the intrinsically lower noise due to the lack of a carrier on resonance. Similar expressions have been developed independently by Shoemaker et. al [37] and Sampas [38].

In practice it is difficult to reach this level of stability due to amplifier noise in the discriminator, residual AM noise in the phase modulators and non-ideal mode-matching into the interferometer.[38] To experimentally determine the performance that can be expected, measurements of the total discriminator noise, ($S_{A,disc}$, or $S_{\nu,disc}$), and slope, (D_A or D_ν), must be made. The ratio of the

two, as described in equation 6, determines the total spectral density of frequency noise that can be expected in closed loop operation. In the following section we describe our frequency stabilization experiments and analyze them using the framework provided by eqns. 1-9.

III. Experiment

A. Apparatus

The Pound-Drever locking scheme used to measure both the spectral density of frequency noise for one laser, and the heterodyne beat note linewidth between two lasers, is shown in Figure 2. The lasers were 40 mW, model 120-03, Lightwave Electronics nonplanar ring oscillators (NPROs). These lasers had PZT frequency actuators attached to the Nd:YAG laser crystals which provided a frequency actuator with an electrical bandwidth of 200 kHz, an actuating coefficient of 1 MHz /V and an electronic tuning range of 20 MHz.

Laser 1 was phase modulated at a frequency of 10.9 MHz, and laser 2 was phase modulated at 20.3 MHz using $LiNbO_3$ phase modulators with a modulation index, β, of 1.1. The two laser beams were then mode matched into a high finesse interferometer (Newport Reasearch Corporation Model SR-150 SuperCavity). The interferometer had a free spectral range (FSR) of 6.327 GHz, a finesse of 22,000 and a transmission passband, $\delta\nu_c$, of 288 kHz. The finesse was measured by phase modulating the laser at a known frequency and comparing the optical transmission width to the known sideband spacing. Typically no more than two higher order transverse modes were measurably excited. The amplitudes of these modes were more than 14 dB below the fundamental, and their frequencies were offset from the axial mode by 0.81 and 1.62 GHz. The phase-modulation sidebands of each laser were well outside the interferometer passband and were therefore completely reflected with essentially no relative phase shift. The polarizing beam splitter (PBS) and quarter-wave plate ($\lambda/4$) served to isolate the reflected and incident beams as well as provide optical isolation of the lasers from their own back reflections.

The NPROs do have a greater tolerance to feedback than standing wave oscillators but are not completely insensitive to it.[20,39] To reach sub-hertz beatnote performance an optical isolator in the

form of a single acousto-optic light modulator was positioned between the beam splitter and the Fabry-Perot reference cavity to provide additional isolation. As the AOM drive frequency was 40 MHz, and the beams propagated through the AOM twice, the optical fields experienced a net frequency shift of 80 MHz before returning to the laser. The 80 MHz frequency shift lies outside of the lockin range associated with these lasers and hence amplitude or frequency instability due to optical feedback was substantially reduced.

The two lasers were also susceptible to mutual injection locking. They could not phase lock however, because they were locked to adjacent axial modes of the interferometer which had a frequency spacing much larger than the laser locking range. Additionally, locking the two lasers to the same interferometer provides common mode rejection against cavity fluctuations.[29]

Near resonance both carriers were reflected from the cavity with a strongly dispersive phase shift. The sidebands, however, were not resonant and therefore reflected from the cavity with no phase shift. When each carrier was mixed with its sidebands at detector D2 an AM term was created with an amplitude proportional to the frequency offset. The amplitude of the AM term was phase sensitively detected in the RF mixer and the output of the lowpass filter was the frequency discriminant error signal. The error signals were amplified by the servos and negatively fed back to the lasers to close both loops and thus maintain lock. The normalized output voltage from each mixer served as the error signal and, as derived in appendix A, eqn. A.12, is given by

$$V_{NOR} = 16F(L/c)J_0(\beta)J_1(\beta)\sqrt{\frac{\mathrm{sinc}^2(x_N/F)}{1+F^2\sin^2(x_N/F)}}\,\delta f_l \qquad (10)$$

where δf_l is the amplitude of the laser frequency fluctuations, L is the length of the interferometer, c is the speed of light, β is the phase modulation index, x_N is the Fourier frequency of the laser frequency fluctuation normalized to the interferometer transmission half-bandwidth, F is the finesse and $F = (2/\pi)F$. In this analysis we have assumed optical impedance matching into the interferometer. In addition, δf_l is assumed to be small compared to the interferometer passband

and higher order terms in the Bessel function expansion are assumed to be negligible. The phase shift ϕ associated with the error signals is also derived in the appendix A and given by

$$\tan(\phi) = -F\tan(\frac{x_N}{F}) \qquad (11)$$

For low noise frequencies the error signal follows the frequency noise and the system behaves as a frequency discriminator. However, for higher frequencies there is a 90° phase shift accompanied by a reduced amplitude in the output voltage (inversely proportional to frequency). In this regime the system behaves as a phase discriminator and the error signal is proportional to the amplitude of the laser phase fluctuation. The transition between the two regimes occurs at a Fourier frequency of half the interferometer bandwidth. Similar expressions for both the phase and amplitude response of the error signals have been discussed elsewhere.[31,37]

The error signals were amplified by high-gain servos that fed back to the PZT frequency actuators bonded directly to the laser crystals. The loop response of the system had a DC gain of 125 dB with a unity gain frequency of 100 kHz. The servos consisted of cascaded integrators together with a lag-lead stage to provide high DC gain as well as the proper slope at the unity gain point. This relatively low gain-bandwidth product is a direct result of the low spectral density of frequency noise associated with these lasers.

B. Spectral density of frequency noise

The NPRO spectral density of frequency noise was measured by using the frequency discrimination of the laser frequency controller used in the stabilization experiments discussed above and shown in Figure 1. Under closed loop operation the linear spectral densities of the noise voltages at the error point, V_{N_e} and the actuator point, V_{N_A}, with units of V/$\sqrt{\text{Hz}}$, can be used to determine the laser spectral density of frequency noise, with units of Hz/$\sqrt{\text{Hz}}$, over a wide bandwidth. These noise voltages are related to the laser noise ($S_{f,laser}$(Hz/$\sqrt{\text{Hz}}$)) by

$$V_{N_e} = \frac{D_v S_{f,laser}}{|1 + KGD_v|} \qquad (12a)$$

and

$$V_{N_A} = \frac{GD_v S_{f,laser}}{|1 + KGD_v|}, \qquad (12b)$$

where D_v is the discriminator slope (in V/Hz), G is the servo gain (in V/V), and K is the actuator coefficient (in Hz/V). The Pound-Drever frequency discriminant has a flat response from DC to the cavity half width ($\delta\nu_c/2$ ~ 144 kHz).[31] The actuator frequency response was flat to ~200 kHz. As a result, from DC to 144 kHz only the servo gains, G(f), in equations 12a and 12b are frequency dependent.

Measurements of the spectral density of noise at the output of the frequency discriminator, the error point N_e, are useful in diagnosing loop performance.[23] This closed loop error signal is the product of the slope of the discriminator and the closed loop spectral density of laser frequency noise. Therefore, spectral analysis of the error signal can be used to obtain information on the gain of the loop, the loop bandwidth, and whether the loop is stable or not. It is also tempting to divide the spectral density of voltage fluctuations at the error point ,V_{N_e}, by the slope of the discriminator,D_V, to determine the closed loop performance of the laser.[36,37] This is misleading however, since the excess noise due to the discriminator is not observed at the error point.[23] Spectral analysis of the error signal can only provide a lower limit on the spectral density of closed loop frequency noise.

The error signal is, however, useful in the analysis of the free running frequency noise of the laser. With a loop gain of less than one, which occurs outside the loop bandwidth, V_{N_e} in equation (12a) is linearly proportional to the intrinsic laser frequency noise ($S_{f,laser}$). Spectral analysis of the error voltage therefore gives information on the spectral density of the free running laser frequency noise for frequencies above the unity gain point. The discriminator noise however, may still be a problem. Since the loop gain is less than one, this noise is additive and sets a lower limit on the sensitivity of the measurement. To overcome this, the system can be calibrated by

adding a known frequency deviation to the laser with the AO modulator and determining the minimum detectable signal. This technique provides an upper limit on the frequency noise of the laser.

Measurements of the spectral density of the free running laser frequency noise are also possible at the actuator point (N_A). With a loop gain much greater than one, which occurs inside the loop bandwidth, V_{N_A} in equation (12b) is also linearly proportional to the intrinsic laser frequency noise ($S_{f,laser}$). This is always the case in any control loop using negative feedback with large loop gains. Spectral analysis of the actuator voltage therefore yields information on the spectral density of the free running frequency noise for frequencies below the unity gain point, assuming of course that the actuator slope, K(V/V), is known. Calibration of the system, as with the error signal, is the best way to determine this slope as well as the minimum sensitivity.

Closed loop spectral density measurements of both the actuator and error signals can therefore be used for wideband measurements of the intrinsic free running laser frequency noise. This information, together with knowledge of the loop gain and excess noise, can be used to calculate the level of closed loop performance that can be expected.

To identify the frequency regimes over which V_{N_e} and V_{N_A} were valid measures of the spectral density and also to calibrate the system, the acousto-optic light modulator (AOM) was driven with the output of a voltage controlled oscillator. A deterministic signal was applied to the AOM which modulated the laser frequency and appeared as a calibration spike in the spectral density of V_{N_e} or V_{N_A}.

A measurement of the detected calibration signal strength as a function of modulation frequency indicated that V_{N_A} was a valid measure of frequency noise from DC to ~4 kHz. As a result, V_{N_e} was used as a measure of the laser frequency noise from 1 kHz to 100 kHz and V_{N_A} as a measurement from 10 Hz to 1 kHz. The sensitivity of this measurement is limited primarily by excess noise in the AOM as well as in the frequency discriminator and was ~0.5 Hz/$\sqrt{\text{Hz}}$ over the low frequency range and ~0.06 Hz/$\sqrt{\text{Hz}}$ from 1 kHz to 100 kHz.

The magnitude of the measured NPRO linear spectral density of frequency noise shown in Figure 3 is smaller than that of other lasers. For instance, at 1 kHz the noise density is ~20 Hz/√Hz for the NPRO whereas it is greater than 10^3 Hz/√Hz and nearly 10^4 Hz/√Hz in typical dye and Ar^+ lasers respectively.[40,41] It is apparent from Figure 3 that the slope of $S_{f,laser}$ at low frequencies is smaller than the slope at high frequencies with a transition region near 1 kHz. A comparison of this work with the work of other authors, who used different techniques, confirmed that this slope change is real.[42-44] The low frequency slope in Figure 3 is ~3 dB/octave and the high frequency slope is 6 dB/octave. The likely explanation of this behavior is thermal filtering of the pump laser amplitude fluctuations. This result will be discussed further in a future publication.[24] The high frequency behavior of the noise was essentially flat with a magnitude of ~0.2 Hz/√Hz and within a factor of 4 of the estimated Schawlow-Townes limit. There has been discussion in the literature that relaxation oscillations would induce laser frequency fluctuations.[45] This, however, was not observed in any of our measurements.

C. 330 mHz Beatnote Linewidth with the Newport Cavity

Figure 4 shows the resultant heterodyne beatnote obtained when independently locking the two lasers to the Newport high finesse cavity. Detector D1 served as a diagnostic port, outside the control loop, that permitted a direct measurement of the relative frequency stability of the two lasers through the heterodyne beat note. The data was obtained by sampling the beatnote waveform for approximately 4 s and Fourier transforming the result with a dynamic signal analyzer.(HP3561A) The long-term drift in the beatnote frequency, which was also seen in the Allan variance measurement reported earlier,[22] limits the ability to improve the resolution of this measurement because as the span decreases, the center frequency does not remain fixed over the increased sampling time.

The resultant, deconvolved linewidth of 330 mHz is still well above the theoretical minimum. The linewidth was measured to be 1.0 Hz and the contribution from the spectrum analyzer was 0.95 Hz. On resonance the detector (D2) photocurrent was ~170 μA, and the inverse

discriminator slope, $1/D_V$, was ~500 kHz/V. The amplifier instrumentation noise was ~15pA/$\sqrt{Hz}$ and the gain of the discriminant was typically between 2800 and 5000 V/A. If these noise terms were the only processes affecting the linewidth of the lasers, then the maximum residual spectral density of frequency noise, $S_{V,disc.}$, would be 0.058 Hz/$\sqrt{Hz}$ corresponding to an amplitude noise limited beatnote linewidth of ~21 mHz.

There are three noise terms that could be degrading the performance: component noise, parasitic etalon effects and Fabry-Perot cavity noise. Component noise, in the experiments described here could occur in either the electro-optic phase modulators or the acousto-optic isolator. Residual amplitude modulation noise in the E-O phase modulator [29,38,46-47] appears as an AM noise term at the modulation frequency and can be interpreted as frequency noise by the discriminators. However, the residual amplitude noise in our phase modulators was measured and appeared to be too small to account for the observed 330 mHz linewidth.

Frequency noise on the drive oscillator in the AOM is convolved directly with the lasers frequency noise spectrum because the AOM shifts the carrier frequency by an amount equal to the instantaneous drive frequency. However, since each laser beam transits the same region of the AOM, both fields experience the same instantaneous drive frequency and so this noise is common mode and should not be observed in the heterodyne beatnote.

Any optical component in the beam path can behave like a low finesse etalon. These parasitic etalons have a frequency dependant phase shift that may add to the phase shift of the Fabry-Perot reference cavity. As the temperature of the optical components changes, this phase shift varies resulting in a shift of the error point and producing frequency noise in the low frequency regime.

The Newport cavity is the likely dominant source of noise. Interferometer length fluctuations change not only the absolute frequency associated with the cavity but also its free spectral range. It is the shift in free spectral range which directly affects the stability of the heterodyne beatnote since both lasers are tightly locked to adjacent axial modes of the reference cavity. Length fluctuations in the interferometer can be caused by acoustic, thermal or seismic noise. Whatever the origin, the shift in free spectral range is related to the length change by

$$\delta\nu_{FSR} = \left(\frac{c}{2L}\right)\left(\frac{\Delta L}{L}\right). \qquad (13)$$

For a fractional length change of 10^{-10} and a FSR of 6.327 GHz the shift in FSR is 633 mHz. Since this effect scales inversely with length, a longer reference cavity would improve frequency stability. Furthermore, if the length of the cavity is increased without affecting the finesse, then the slope of the discriminant also increases due to the longer photon storage time and smaller cavity linewidth.

D. Locking to the Stanford high finesse interferometer

In an attempt to take advantage of the improved discrimination obtainable with a longer cavity we built an interferometer using two mirrors from a Newport SuperCavity and a 22 cm long cylindrical quartz spacer. A photograph of this cavity is shown in Figure 5. There was some concern that as the length of the cavity increased the larger mode diameter on the mirrors would lower the finesse. These fears were unfounded. The finesse of this interferometer was measured to be 27,500. The finesse of the fixed length interferometer was measured by rapidly tuning the laser frequency across the optical bandpass of the interferometer and measuring the photon cavity lifetime. A photon lifetime of 6.4 μsec was measured which corresponds to a cavity bandpass of 25 kHz and a finesse of 27,500. We believe this to be the narrowest optical bandpass of any 1064 nm Fabry-Perot.

The beat note experiment was repeated using this interferometer in place of the Newport Supercavity and resulted in a beatnote linewidth of 700 mHz, as shown in Figure 6. The increase in the beatnote linewidth is most likely a result of the acoustic, thermal and seismic noise on the longer quartz spacer which was mounted in air. This result is consistent with the hypothesis that the interferometer length fluctuations caused by the lab environment set the current limit to the linewidth.

IV. Conclusion

The relative stability of two 40 mW Nd:YAG NPROs has reached 330 mHz using Pound-Drever locking to a high finesse Fabry-Perot. In addition, a Fabry-Perot interferometer with an optical bandwidth of 25 kHz, a FSR of 680 MHz and a finesse of 27,500 has been built and current improvements in mirror technology suggest that it will soon be possible to build interferometers with still narrower bandwidths. While this result is, to date, the narrowest heterodyne beatnote linewidth reported for frequency stabilized diode laser pumped solid state lasers, improvements are needed to reach the quantum limit.

The authors wish to thank Professor John Hall, Yekta Gersel, Professor M.M. Fejer, A.D. Farinas, and N. Sampas for helpful discussions. This research was supported by the National Science Foundation and the NASA SUNLITE program.

Appendix A. Frequency response and discriminant slope of the Pound-Drever error signal

The straightforward method of attacking the problem of the frequency response of the Pound-Drever error signal is to model the laser field as a carrier frequency, ω_0, which is resonant with the optical cavity, together with a sinusoidal noise contribution at a frequency ω_N away from line center. The mixer output (the error signal) dependence on ω_N is then developed. With the carrier modeled in this way the electric field of the laser can be described as

$$E = E_i e^{j(\omega_0 t + \alpha \sin\omega_N t)} \qquad (A.1)$$

where E_i is the amplitude of the incident field. The instantaneous frequency of the laser is defined as the time derivative of the phase of the electric field, $\Omega(t) = \omega_0 t + \alpha\sin\omega_N t$, and is given by

$$\frac{1}{2\pi}\frac{d\Omega}{dt} = \nu_o + \alpha\nu_N \cos(\omega_N t) \qquad (A.2)$$

where units of Hz are used to be consistent with the units of the control elements.

The laser carrier with its noise contribution is then phase modulated at a frequency ω_m. The modulated carrier plus noise sidebands is given by

$$E = E_i e^{j(\omega_0 t + \alpha\sin\omega_N t + \beta\sin\omega_m t)} \qquad (A.3a)$$

which, using an expansion in Bessel functions, can be approximated as

$$E \approx E_i\left[J_0(\beta) + \frac{J_0(\beta)\,\alpha}{2}\left(e^{j\omega_N t} - e^{-j\omega_N t}\right) + J_1(\beta)\left(e^{j\omega_m t} - e^{-j\omega_m t}\right)\right] e^{j\omega_0 t} \,. \qquad (A.3b)$$

In this expression J_0 and J_1 are the Bessel functions of order 0 and 1, β is the phase modulation index and $J_1(\alpha) \sim \alpha/2$ is assumed for simplicity. The higher harmonics of the modulation frequency are assumed to be negligible in equation (A.3b) and the noise contributions at ($\omega_m \pm \omega_N$) are ignored since they cannot effect the AM contribution to the photo-diode output at ω_m.

The electric field of the laser is incident on the high finesse interferometer and the ratio of reflected to incident field is given by

$$\frac{E_T}{E_i} = \left[J_0(\beta)F(0) + \frac{J_0(\beta)\,\alpha}{2}\left(C(\theta_N)\,e^{j\omega_N t} - C^*(\theta_N)\,e^{-j\omega_N t}\right) + J_1(\beta)\,2j\sin(\omega_m t)\right] e^{j\omega_0 t}\,. \tag{A.4}$$

$C(\theta_N)$ is the complex field reflection coefficient of the cavity,[35]

$$C(\theta_N) = \frac{R_1 - Re^{j\theta_N}}{\sqrt{R_1}\left(1 - Re^{j\theta_N}\right)}\,, \tag{A.5a}$$

where

$$\theta_N = \frac{2\omega_N L}{c} \tag{A.5b}$$

and

$$R = \sqrt{R_1 R_2}\,e^{-\alpha_i L} \tag{A.5c}$$

with front mirror reflectivity R_1, back mirror reflectivity R_2, loss coefficient $\alpha_i(cm^{-1})$, and mirror separation L. The modulation sidebands are assumed to lie well outside the cavity passband in equation (A.4) and therefore $C(\theta_m) = 1$.

The normalized photo-diode output voltage is given by

$$V_{NOR} = \frac{E_T E_T^*}{E_i^2} = \frac{P_T}{P_i} \tag{A.6}$$

which contains terms at DC, $2\omega_N$, and $2\omega_m$; as well as the term of interest at ω_m. The mixer and low pass filter isolate the term at ω_m which is given by

$$\begin{aligned} V_{NOR}(\omega_m) &= -j\,2\alpha\,J_0(\beta)\,J_1(\beta)\left[C(\theta_N)\,e^{j\omega_N t} - C^*(\theta_N)\,e^{-j\omega_N t}\right]\sin(\omega_m t) \\ &= 4\alpha\,J_0(\beta)\,J_1(\beta)\,\mathrm{Im}\left[C(\theta_N)\,e^{j\omega_N t}\right]\sin(\omega_m t)\,. \end{aligned} \tag{A.7}$$

Equation A.7 can be written to more clearly indicate the magnitude and phase response of the modulation envelope as

$$V_{NOR}(\omega_m) = 4\alpha\, J_0(\beta)\, J_1(\beta) \left| C(\theta_N) \right| \cos(\omega_N t + \phi) \sin(\omega_m t) \qquad \text{(A.8a)}$$

where

$$\tan(\phi) = - \frac{\mathrm{Re}\, C(\theta_N)}{\mathrm{Im}\, C(\theta_N)} . \qquad \text{(A.8b)}$$

The normalized output of the lowpass filter ignoring loss is therefore

$$V_{out} = 4\alpha\, J_0(\beta)\, J_1(\beta) \left| C(\theta_N) \right| \cos(\omega_N t + \phi) , \qquad \text{(A.9a)}$$

where the magnitude of the complex field reflectivity, from equation (A.5a), is given by

$$\left|C(\theta_N)\right| = \sqrt{\frac{F^2 \sin^2(\theta_N)}{1 + F^2 \sin^2(\theta_N)}} . \qquad \text{(A.9b)}$$

A normalized noise frequency can be defined as

$$x_N \equiv \frac{2\nu_N}{\delta\nu_c} , \qquad \text{(A.10)}$$

which, together with equation (A.5b), can be substituted into equations (A.9) to obtain

$$V_{out} = 16F(L/c)\, J_0(\beta)\, J_1(\beta) \sqrt{\frac{\mathrm{sinc}^2(x_N/F)}{1 + F^2 \sin^2(x_N/F)}}\, \alpha\nu_N \cos(\omega_N t + \phi) \qquad \text{(A.11a)}$$

where

$$\tan(\phi) = - F \tan(x_N/F) . \qquad \text{(A.11b)}$$

In these equations F is the interferometer finesse, $\delta\nu_c = (c/2LF)$ is the interferometer linewidth and $F = (2/\pi)F$. Also, $R_1 = R$ (impedance matching) is assumed for simplicity. From equation A.2 it is seen that the amplitude of the frequency deviation of the noise input is $\alpha\nu_N$. Therefore, the slope of the error signal (with units of Hz^{-1}) can be identified as

$$\text{slope } (\text{Hz}^{-1}) = 16F(L/c)J_0(\beta)J_1(\beta)\sqrt{\frac{\text{sinc}^2(x_N/F)}{1+F^2\sin^2(x_N/F)}} \quad . \qquad \text{(A.12)}$$

This slope is maximized for $\beta \sim 1.08$ which, when substituted into equation A.12, gives

$$\text{slope}_{max} \ (\text{Hz}^{-1}) = \frac{8J_0(\beta)J_1(\beta)}{\delta\nu_c} \sim \frac{2.71}{\delta\nu_c} \ (\beta = 1.08) \qquad \text{(A.13)}$$

in the vicinity of $x_N = 0$.

The discriminator slope (D_W) in units of W/Hz is the product of the normalized slope and the incident power, P_i, as described in equation (A.6). It is useful, however, to define the discriminant slope in units of V/Hz, D_V as in equation (4), or A/Hz, D_A . These are given by

$$D_v(\text{V/Hz}) = \frac{8J_0(\beta)J_1(\beta)}{\delta\nu_c} R_vP_i \qquad \text{(A.14a)}$$

and

$$D_A(\text{A/Hz}) = \frac{8J_0(\beta)J_1(\beta)}{\delta\nu_c} \frac{e\eta P_i}{h\nu} \qquad \text{(A.14b)}$$

where R_V is the photo-detector responsivity in V/W, η is the detector quantum efficiency, and e is the charge of an electron.

A comparison of equation A.11 with A.12 demonstrates that the error signal is in phase with the input noise signal at low noise frequencies. For noise frequencies that are large compared to the cavity half width however, the slope of the error signal is reduced and the phase shift approaches -90°. In this regime the discriminator behaves as a frequency integrator or phase detector. However, with a simple phase advance of +90° in the servo electronics, the response of the system can be maintained to frequencies that are large compared to the cavity bandwidth. This is in marked contrast to the transmission case which is plagued by time delays in the control loop[33] rather than a simple phase shift.

Equation A.11 describes the frequency response of the discriminator. Furthermore, it demonstrates the improvement that can be achieved when using the Pound-Drever discrimination technique as opposed to fringe side locking. Similar results have been discussed elsewhere (Drever, Schoemaker, Sampas, Houssin) but the derivation presented here has not.

References

1. R.L. Byer,"Diode laser-pumped solid-state lasers," *Science*, **239**,742-747 (1988).

2. T.Y. Fan and R.L. Byer,"Diode laser-pumped solid-state lasers," *IEEE J. Quantum Electron.*, **24**, 895-912 (1988)

3. K. Wallmeroth and R. Letterer, "Cesium frequency standard for lasers at λ = 1.06 μm," *Opt. Lett.* **15**, 812-814 (1990).

4. T. Day, A.D. Farinas and R.L. Byer,"Demonstration of a low bandwidth 1.06 mm optical phase-locked loop for coherent homodyne communication," *IEEE Photon. Techn. Lett.*, 2, 294-296 (1990).

5. L. G. Kazovsky, "Balanced phase-locked loops for optical homodyne receivers: Performance analysis, design considerations, and laser linewidth requirements," *J. Lightwave Technol.*, **LT-4**, 182-195 (1986).

6. T.J. Kane, W, J. Kozlovsky, Charles E. Bivik,"Coherent laser radar at 1.06μm using Nd:YAG lasers," *Opt. Lett.* **12**, 239-241, April 1987.

7. A. C. Nilsson, T. Day, A. D. Farinas, E. K. Gustafson, and R. L. Byer, "Narrow linewidth operation of diode-laser-pumped nonplanar ring oscillators," (Springer Verlag Topics in Physics: Proceedings of Fourth Symposium on Frequency and Metrology, Ancona Italy, 1988).

8. K.S. Thorne, *300 Years of Gravitation* ed. S.W. Hawking and W. Israel, Cambridge University Press, 1987.

9. S. Kawamura, J. Mizuno, J. Hirao, N. Kawashima, and R. Schilling, "10m Prototype for the laser interferometer gravitational antenna," The institute of space and astronautical science, Tokyo, Report # 637 (1989).

10. W.J. Kozlovsky, C.D. Nabors, and R.L. Byer,"Efficient second harmonic generation of a diode-laser-pumped CW Nd:YAG laser using monolithic MgO:LiNbO3 external resonant cavities," *IEEE J. Quantum Electron.*, **24**, 913-919 (1988).

11. W.J. Kozlovsky, C.D. Nabors, R.C. Eckardt, and R.L. Byer,"Monolithic MgO:LiNbO3 doubly resonant optical parametric oscillator pumped by a frequency-doubled diode-laser-pumped Nd:YAG laser," *Opt. Lett.*, **14**, 66-68 (1989).

12. C.D. Nabors, R.M. Shelby,"Two-color squeezing and sub-shot-noise signal recovery in doubly resonant optical parametric oscillators," *Phys. Rev. A*, **42**, 556-559 (1990).

13. P. Bender, "Proceedings of the workshop on technologies for a laser gravitational wave observatory in space," Annapolis, Md., Ed. R. Hellings, JPL Report

14. R.D. Reasenberg, R.W. Babcock, J.F. Chandler, M.V. Gorenstein, J.P. Huchra, M.R. Pearlman, I.I. Shapiro, R.S. Taylor, P. Bender, A. Buffington, B. Carney, J.A. Hughes, K.J. Johnson, B.F. Jones, L.E. Matson,"Microarcsecond optical astrometry: An instrument and its astrophysical applications," *Astron. J.* , 1731-1745 (1988).

15. B. Schumaker, "Scientific applications of frequency-stabilized laser technology in space," JPL Report No. 90-50, (1990).

17. D. Hils, J.E. Faller, and J.L. Hall,"Practical sound reducing enclosure for laboratory use," *Rev. Sci. Instrum.*, **87**, 2532-2534 (1986).

18. T. J. Kane and R. L. Byer, "Monolithic, unidirectional single-mode Nd:YAG ring laser," *Opt. Lett.*, **10**, 65-67 (1985).

19. T. J. Kane, A. C. Nilsson, and R. L. Byer, "Frequency stability and offset locking of a laser-diode-pumped Nd:YAG monolithic nonplanar ring oscillator," *Opt. Lett.*, **12**, 175-177 (1987).

20. A. C. Nilsson, "Eigenpolarization theory and experimental linewidth study of monolithic nonplanar ring oscillators," Ph.D. dissertation, Dept. of Applied Physics, Stanford University, Stanford California, 1989.

21. T. Day, A. C. Nilsson, M. M. Fejer, A. D. Farinas, E. K. Gustafson, C. D. Nabors, and R. L. Byer, " 30-Hz linewidth, diode-laser-pumped, Nd:GGG nonplanar ring oscillators by active frequency stabilization," *Electron. Lett.*, **25**, 810-812 (1989).

22. T. Day, E. K. Gustafson, and R. L. Byer, "Active frequency stabilization of a 1.062 μm, Nd:GGG, diode-laser-pumped nonplanar ring oscillator to less than 3 Hz of relative linewidth," *Opt. Lett.*, **15**, 221-223 (1990).

23. J. L. Hall, "Stabilizing lasers for applications in quantum optics," in *Quantum Optics IV*, ed. by J. D. Harvey and D. F. Walls (Springer Verlag: Proceedings of the Fourth International Conference, Hamilton New Zealand ,1986).

24. T. Day," Spectral density of frequency noise in diode laser pumped nonplanar ring lasers," To be published.

25. A. Yariv, *Optical Electronics 3rd Ed.*(New York: CBS College Publishing 1985).

26. D. S. Elliot, R. Roy, and S. J. Smith, "Extracavity laser band-shape and bandwidth modification," *Phys. Rev. A*, **26**, 12-18 (1982).

27. T. J. Kane, "Coherent laser radar at 1.06μm using solid state lasers", Ph.D. dissertation, Dept of Electrical Engineering, Stanford University, Stanford California, 1989.

28. L. G. Kazovsky, "Performance analysis and laser linewidth requirements for optical PSK heterodyne communications systems," *J. Lightwave Technol.*, **LT-4**, 415-425 (1986).

29. Ch. Salomon, D. Hils, and J. L. Hall, "Laser stabilization at the millihertz level," *J. Opt. Soc. Am. B*, **5**, 1576-1587 (1988).

30. R. L. Barger, M. S. Sorem, and J. L. Hall, "Frequency stabilization of a cw dye laser," *Appl. Phys. Lett.*, **22**, 573-575 (1973).

31. R. W. P. Drever, J. L. Hall, F. V. Kowalski, J. Hough, G. M. Ford, A. J. Munley, and H. Ward, "Laser phase and frequency stabilization using an optical resonator," *Appl. Phys. B*, **31**, 97-105 (1983).

32. A.D. White, "Frequency stabilization of gas lasers," A.D. White, *IEEE J. Quant. Elect.*, Vol. QE-1, No.8, November 1965.

33. J. Helmcke, S. A. Lee, and J. L. Hall, "Dye laser spectrometer for ultrahigh spectral resolution: design and performance," *Appl. Opt.*, **21**, 1686-1694 (1982).

34. Y. V. Troitskii, "Optimization and comparison of the characteristics of optical interference discriminators," *Sov. J. Quantum Electron.*, **8**, 628-631 (1978).

35. Anthony E. Siegman, *Lasers*, Ch. 11, (Mill Valley: University Science Books, 1986).

36. M. Ohtsu, M. Murata, and M. Kourogi, "FM noise reduction and subkilohertz linewidth of an AlGaAs laser by negative electrical feedback," *IEEE J. Quantum Electron.*, **26**, 231-241 (1990).

37. D. Shoemaker, A. Brillet, C. N. Man, O. Cregut, and G. Kerr, "Frequency-stabilized laser-diode-pumped Nd:YAG laser," *Opt. Lett.*, **14**, 609-611 (1989).

38. N. Sampas Ph.D. dissertation, Dept. of Physics, "A Ring Gyroscope with optical subtraction," University of Colorado, Boulder Colorado, 1990.

39. A. C. Nilsson, E. K. Gustafson, and R. L. Byer, "Eigenpolarization theory of monolithic nonplanar ring oscillators," *J. Quantum Elec.*, **25**, 767-790 (1989).

40. R. Kallenbach, C. Zimmermann, D. H. McIntyre, and T. Hansch, "A blue dye laser with sub-kilohertz stability," *Opt. Comm.*, **70**, 56-60 (1989).

41. M. Houssin, M Jardino, B. Gely, and M. Desaintfuscien, "Design and performance of a few-kilohertz-linewidth dye laser stabilized by reflection in an optical resonator," *Opt. Lett.* , **13**, 823-825 (1988).

42. P. Fritschel, A. Jeffries, and T. Kane, "Frequency fluctuations of a diode-pumped Nd:YAG ring laser," *Opt. Lett.* , **14**, 993-995 (1989).

43. K. J. Williams, A. Dandridge, A. D. Kersey, J. F. Weller, A. M. Yurtek, and A. B. Tveten, "Interferometric measurement of low-frequency phase noise characteristics of diode laser-pumped Nd:YAG ring laser," *Electron. Lett.*, **25**, 774-776 (1989).

44. T. J. Kane Ligthwave Electronics, 1161 San Antonio Rd., Mt. View, CA 94043 private communication.

45. L. G. Kazovsky, and D. A. Atlas, "A 1320 nm experimental optical phase-locked loop," *IEEE Photonics Technology Letters*, **1**, 395-397 (1989).

46. N. C. Wong, and J. L. Hall, "Servo control of amplitude modulation in frequency-modulation spectroscopy: demonstration of shot-noise-limited detection," *J. Opt. Soc. Am. B*, **2**,1527-1533 (1985).

47. E. A. Whittaker, M. Gehrtz, and G. C. Bjorkland, "Residual amplitude modulation in laser electro-optic phase modulation," *J. Opt. Soc. Am. B.*, **2**, 1320-1326 (1985).

Captions

Figure 1. Laser frequency stabilization cast as a problem in control theory showing: 1) the plant (the laser), 2) the frequency discriminator (interferometer) , 3) the servo, and 4) frequency actuator (PZT glued on the ring laser). To model the problem excess noise is added at the output of each control element. The actuator and laser noise contributions are represented by $S_{f,laser}$. The frequency discriminator noise is represented by $S_{f,disc}$ and the servo noise by $S_{f,servo}$. The actuator and error points can be used to measure the spectral density of frequency noise of the free running laser.

Figure 2. Schematic diagram of the dual laser locking experiment using two 40 mW, 1064 nm, Lightwave Electronics Model 120-03 NPROs independently Pound-Drever locked in reflection to adjacent axial modes (spaced 6.327 GHz apart) of a 22,000 Finesse Newport Inc. Model SR-150-C interferometer.

Figure 3. The spectral density of frequency noise for a 40 mW, diode laser pumped NPRO obtained by using the frequency discrimination of the laser frequency controller.

Figure 4. A 330 mHz heterodyne beatnote linewidth, measured with an HP 3561A dynamic signal analyzer, when two NPROs were independently Pound-Drever locked to adjacent axial modes of the same Newport Inc. SuperCavity.

Figure 5. Photograph of the Stanford high finesse 1064 nm interferometer. The interferometer has a free spectral range of 680 MHz, a finesse of 27,500 and an optical passband of 25 kHz.

Figure 6. A 700 mHz heterodyne beatnote linewidth obtained by locking to the Stanford high finesse interferometer.

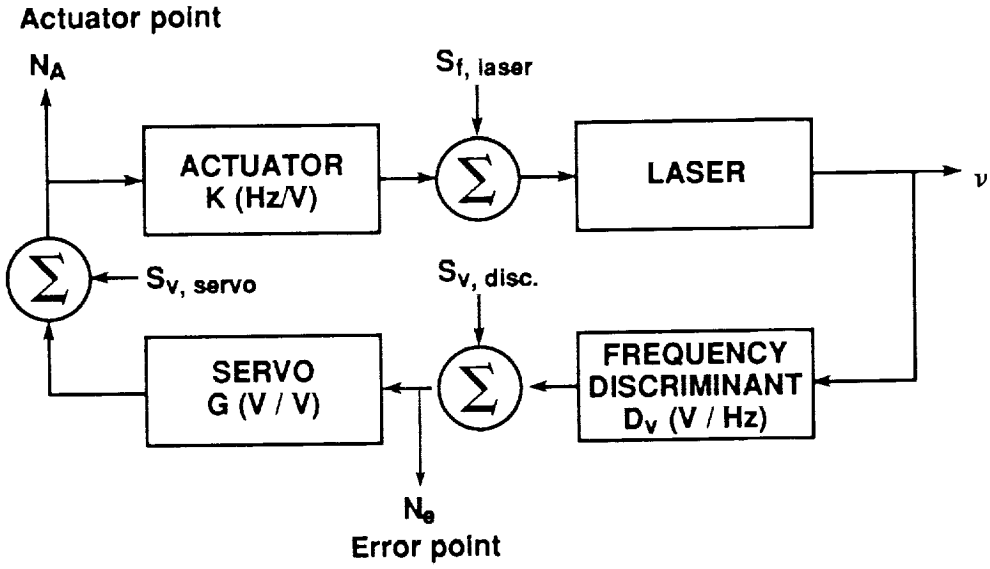
Actuator point
N_A
$S_{f,\ laser}$
ACTUATOR
K (Hz/V)
LASER
ν
$S_{v,\ servo}$
$S_{v,\ disc.}$
SERVO
G (V / V)
FREQUENCY
DISCRIMINANT
D_v (V / Hz)
N_e
Error point

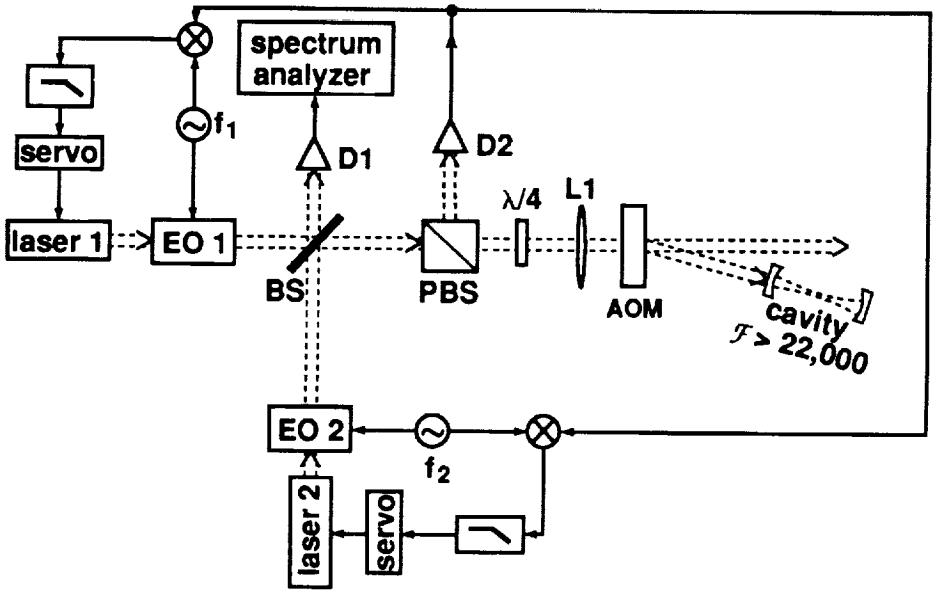
spectrum analyzer
servo
laser 1
EO 1
f_1
D1
D2
BS
PBS
λ/4
L1
AOM
cavity
$\mathcal{F}$ > 22,000
EO 2
f_2
laser 2
servo

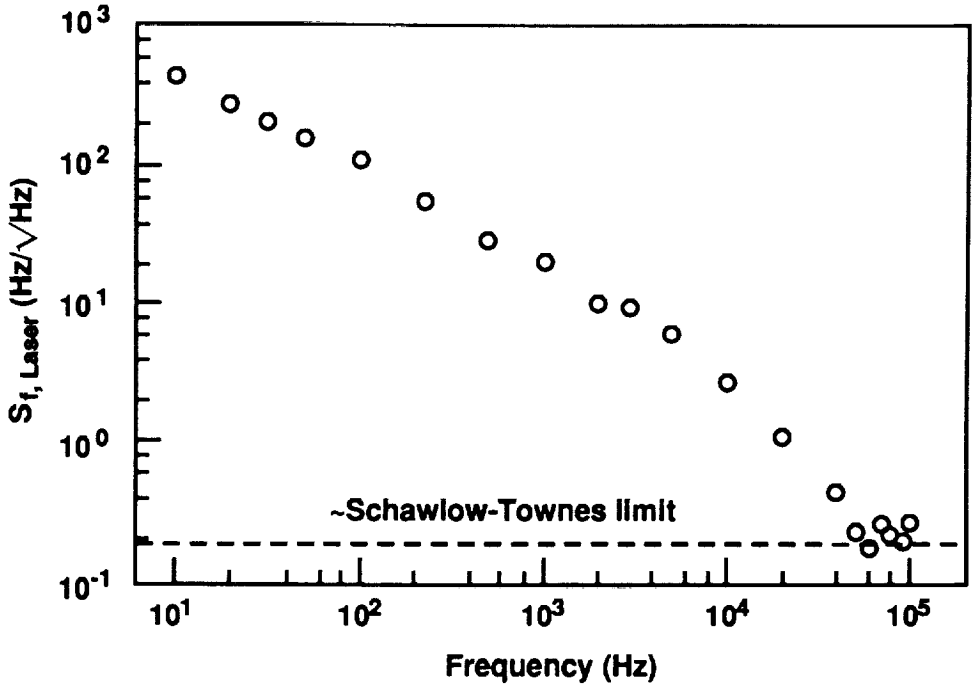
10^3
10^2
10^1
10^0
10^{-1}
$S_{f,\,Laser}$ (Hz/$\sqrt{}$Hz)
~Schawlow-Townes limit
10^1
10^2
10^3
10^4
10^5
Frequency (Hz)

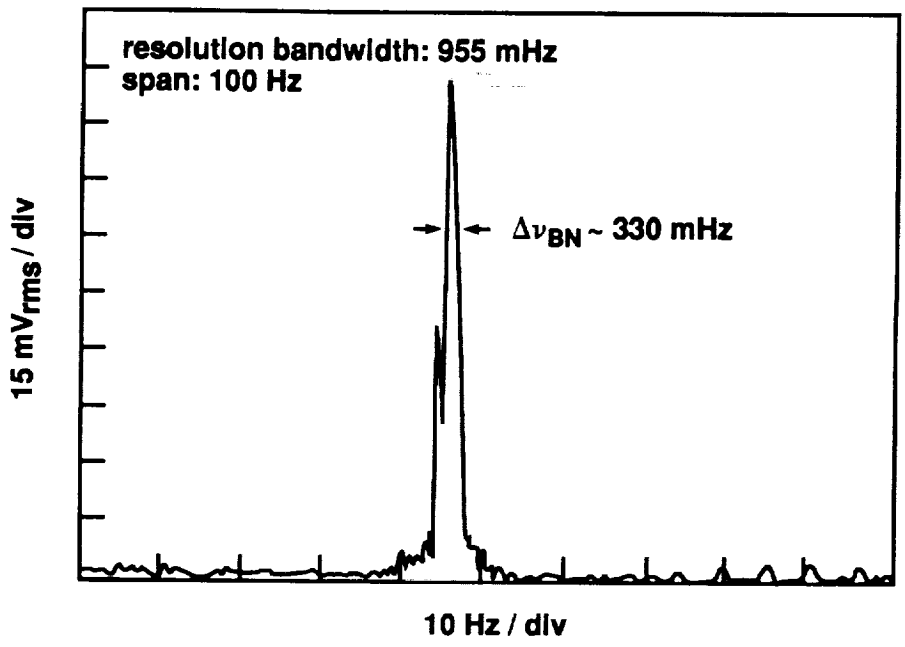
resolution bandwidth: 955 mHz
span: 100 Hz
$\Delta\nu_{BN}$ ~ 330 mHz
15 mV_{rms} / div
10 Hz / div

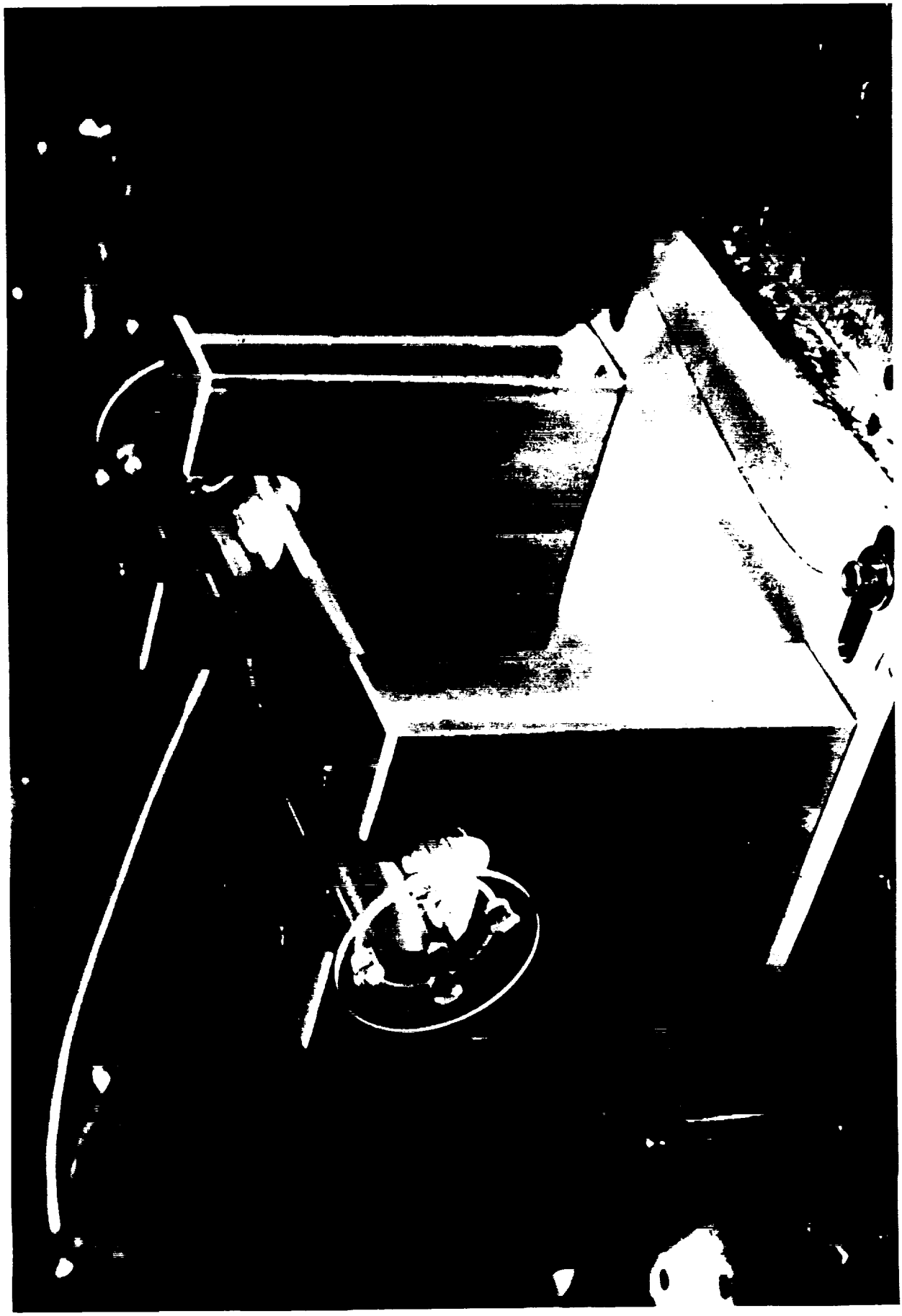

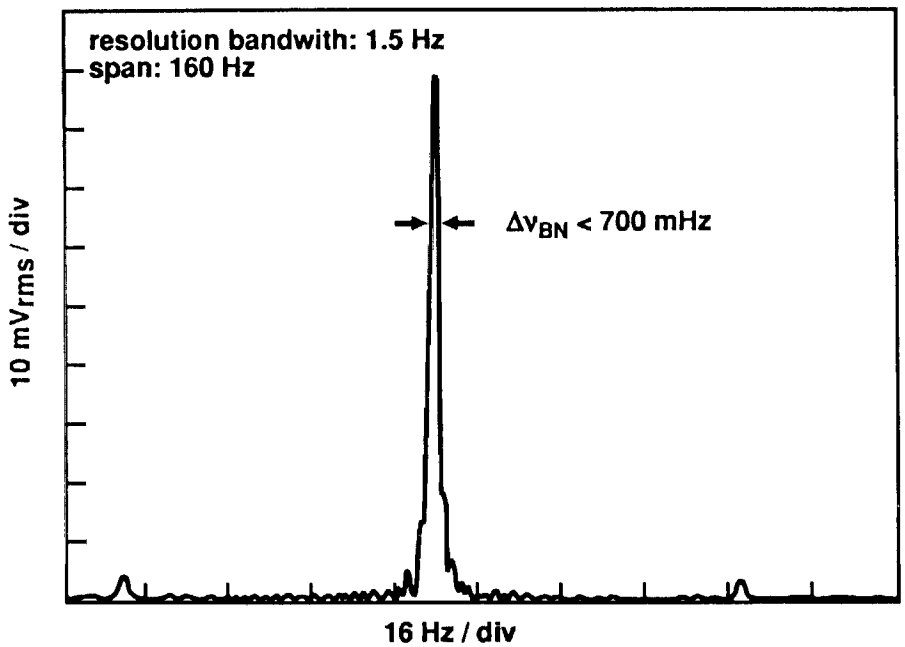
resolution bandwith: 1.5 Hz
span: 160 Hz
$\Delta\nu_{BN}$ < 700 mHz
10 mVrms / div
16 Hz / div